

Quantifying the Surface Coverage of Conjugate Molecules on Functionalized Nanoparticles

Leonard F. Pease III,[†] De-Hao Tsai,^{†,‡} Rebecca A. Zangmeister,[†] Michael R. Zachariah,^{*,†,‡} and Michael J. Tarlov^{*,†}

National Institute of Standards and Technology (NIST), 100 Bureau Drive MS 8362, Gaithersburg, Maryland 20899, and The University of Maryland, 2181 Glenn L. Martin Hall, College Park, Maryland 20742

Received: July 16, 2007; In Final Form: August 31, 2007

Here we present a method to determine the surface coverage or surface density of biological molecules conjugated to nanoparticle surfaces. Electrospray-differential mobility analysis (ES-DMA) is used to determine a coating thickness by measuring the change in the size of gold nanoparticles before and after modification with thiol-derivatized single-stranded DNA. The DNA surface coverage is then obtained from the coating thickness through the use of a simple random coil model. The method requires neither fluorescent tagging nor calibration curves. We believe ES-DMA to be a broadly applicable nanometrology tool for the characterization of biologically conjugated nanoparticles.

This letter addresses a key problem in nanoscience and nanotechnology: how to determine the molecular surface coverage of nanoparticles derivatized with organic or biological molecules, particularly those without a fluorescent tag. Many approaches to functionalize engineered particles have been developed, but characterizing the number of moieties dotting the surface of a nanoparticle remains a critical technical challenge and a major barrier to commercial development. For example, measuring surface coverage will be key to the development, manufacturing, quality control, and regulatory approval of nanobiomaterials for therapeutic use. Additionally, surface coverage measurements will aid quantitative understanding of the results from nanoparticle sensors, enable engineering of particles for energy applications, and facilitate nanoparticle toxicology studies. Here we demonstrate the use of electrospray-differential mobility analysis (ES-DMA) to determine the surface coverage of semiflexible molecules on nanoparticles by measuring changes in particle size.

To demonstrate our approach, we select gold nanoparticles coated with single-stranded DNA (ssDNA), which hold potential for a variety of uses ranging from cancer treatments to genetic diagnostics.^{1–5} Comparing the diameter of coated and bare particles determines how far the ssDNA protrudes from the surface. We then develop a simple random coil model to approximate the projected area and volume occupied by an individual strand. The surface coverage then follows from the molecular footprint.

In differential mobility analysis, also referred to as gas-phase electrophoretic mobility molecular analysis (GEMMA),^{6,7} a particle suspension must be conveyed first into the gas phase. Electrospray ionization suits this purpose well, producing a narrow distribution of droplet diameters. The droplets pass

through a neutralizing chamber where collisions with charged ions reduce the charge to a modified Boltzmann distribution.⁸ Consequently, the particles analyzed in the DMA carry predominantly a single net positive charge. As the droplets containing a gold nanoparticle dry, any salts or other nonvolatile impurities encrust the surface. As only a small fraction of droplets contain gold particles, most particles entering the DMA are simply dried salts. Within the analysis chamber, charged particles are attracted to a center electrode while being dragged along by a carrier gas. Particles for which the radial electrical force balances the radial drag force pass through a collection slit in the center electrode. The drag force in the free molecular regime depends on the projected area; this is a fact we employ in our model for surface coverage. Finally, a condensation particle counter enumerates the number of particles passing through the detector per cubic centimeter of gas flow. Stepping through the voltage yields a particle size distribution. In this manner, particles with diameters greater than 3 nm may be sized with high precision. For example, for nominally 10 nm Au nanoparticles, the standard deviation of the number-average diameter is ± 0.1 nm.

Figure 1 displays two ion mobility spectra: one (red) acquired from a solution containing bare Au nanoparticles nominally 20 nm in diameter and the other (blue) from a solution of 20 nm Au nanoparticles coated with thiol-modified ssDNA [(dT)₂₀-SH], where dT represents deoxythymine and the subscript denotes the number of bases per strand. Typical ion mobility spectra display two peaks. The first set of peaks (<10 nm) corresponds to salt particles that result from the drying of droplets not containing Au particles. Their location depends on the concentration of nonvolatile salts present in the droplets prior to drying, which can vary modestly with sample preparation. The second set of peaks (>15 nm) represents Au particles, one bare and the other modified with (dT)₂₀-SH, both encrusted with any nonvolatile salts. Because droplets with and without a gold particle have the same initial size, the thickness contributed by

* To whom correspondence should be addressed. (M.J.T) Phone: 301-975-2058. Fax: 301-375-2643. E-mail: michael.tarlov@nist.gov. (M.R.Z.) Phone: 301-405-4311. Fax: 301-314-9477. E-mail: mrz@umd.edu.

[†] National Institute of Standards and Technology (NIST).

[‡] The University of Maryland.

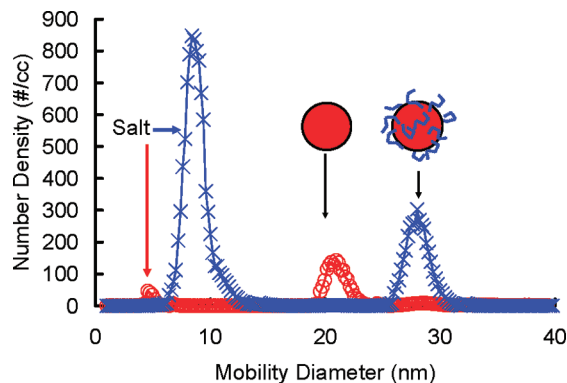


Figure 1. Two typical particle size distributions of nominally 20 nm Au particles, one bare (○) and the other coated with (dT)₂₀-SH (×). The difference between the two particle size distributions determines the apparent coating thickness.

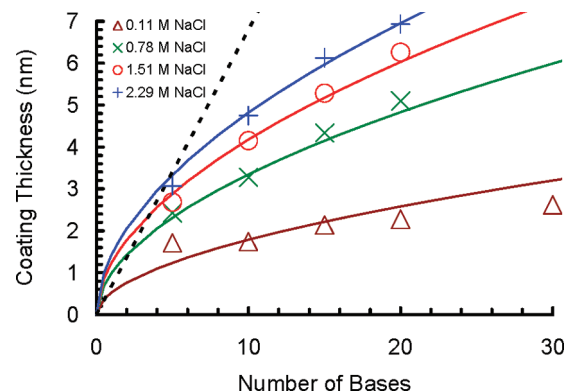


Figure 2. Apparent coating thickness, H , versus number of dT nucleotides per strand, N_b , for a variety of salt concentrations, n_s . The dashed and solid lines respectively represent fits for a contour length model for fully stretched out DNA versus that of a square root dependence [$H = 1.1N_b^{0.53}n_s^{0.35} \text{ nm L}^{0.35} \text{ mol}^{-0.35}$] characteristic of strands coiled into low-grafting density layers (see text).

the shells of dry nonvolatile salts can be removed by subtracting the volume of the salt particle from that of the nanoparticle similar to the work of Kaufman.⁹ The narrow distribution in droplet size produced by the electrospray minimizes uncertainty associated with this correction. Data in subsequent figures reflect this correction. Subtraction of the diameter of the bare particle from the DNA-coated nanoparticle determines the apparent coating thickness, H , presented in Figure 2, which is twice the thickness of the coating layer on either side of the particle.

Using ES-DMA, we investigated the dependence of the coating thickness on the number of dT nucleotides within a ssDNA strand, N_b , and the salt concentration, n_s . The dependence of the coating thickness on the number of bases per strand is related to the spatial configuration of the bases within the strand in the dry state. If the strands pack together tightly in a brush structure, similar to alkanethiol self-assembled monolayers, then the bases will extend into configurations that minimize interstrand repulsion. Accordingly, the coating thickness should scale linearly on the contour length (i.e., the length of the ssDNA backbone), such that $H \sim N_b$. However, if packing allows for sufficient space between the strands, the bases will adopt a random coil configuration to maximize entropy (appropriate for dried strands), and then the coating thickness should be proportional to the linear end-to-end distance, $\langle x^2 \rangle^{1/2}$, of a strand. For freely jointed Gaussian chains, $\langle x^2 \rangle^{1/2} = cN_b^{1/2}N_k^{1/2}l_b$, where N_k represents the number of bases per Kuhn length ($l_k = N_k l_b$), l_b describes the length of a base, and $c = 0.62$ for end-tethered strands on a hard sphere with minimal surface attraction

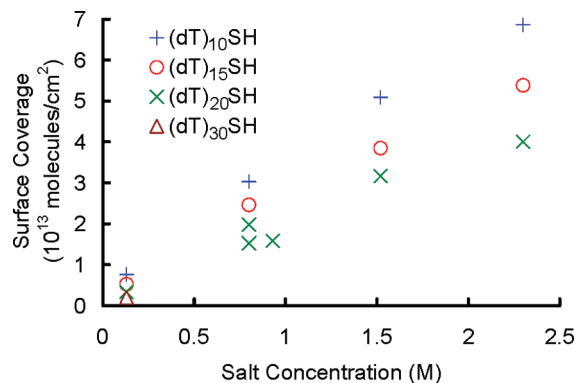


Figure 3. The surface coverage, σ , versus the salt concentration of the ssDNA solution in which the particles were immersed during preparation. Shorter strands display higher surface coverages because each strand occupies a smaller footprint.

[appropriate for oligo(dT) strands on gold],¹⁰ though a variety of prefactors remain available to account for surface-strand interactions.¹¹ Accordingly, we expect $H \sim N_b^{1/2}$, and indeed Figure 2 shows square root scaling to fit the data well. We thus conclude that the strands adopt a random coil configuration on the nanoparticle surface.^{11–13} Consequently, the coating does not meet the formal requirements for a polymer brush, though the DNA community often refers informally to these surface coatings as brushes.¹⁴

Knowing the configuration of the strands enables estimation of the surface coverage. Here we note that while the structure of the strands may change upon drying, the surface coverage does not. The drag force experienced by the coated particle in the DMA depends on the diameter of the particle, D , the projected area of the coiled strands characterized by $\langle x^2 \rangle^{1/2}$, and the surface coverage, σ . Knowing D and $\langle x^2 \rangle^{1/2}$ allows inference of σ from the data with a suitable model. We derive an analytical expression for the drag force for a “lumpy sphere” model in which the ssDNA occupies N_m hemispherical caps of radius $\langle x^2 \rangle^{1/2}$, where N_m represents the number of caps around the two dimensional projection of the particle’s circumference (see Supporting Information).¹⁵ The apparent coating thickness, H , determines N_m , which gives a measure of a strand’s footprint. The surface coverage, consequently, may be approximated as $\sigma = [(D + H)^2 - D^2]/[2\pi D \langle x^2 \rangle^{1/2}]$.² Using this model, we find σ ranges between 2.0×10^{12} and 6.9×10^{13} strands/cm² as displayed in Figure 3, assuming $l_b = 0.59 \text{ nm}$ and $N_k = 3$ ($l_k = 1.8 \text{ nm}$) for $N_b = 10\text{--}30$ bases.^{16,17} By comparison, “brushes” prepared under similar conditions have reported coverages from 1.0×10^{13} to 2.0×10^{13} strands/cm² for 12 mers on nanoparticles and 4.0×10^{12} to 2.5×10^{13} strands/cm² for 25 mers on planar substrates in reasonable agreement with the values derived from our model.^{3–5,18}

An alternative approach approximates the surface coverage if the bulk density is known. Here the number of strands on the particle equals the ratio of the volume of the shell containing the DNA, $\pi[(D + H)^3 - D^3]/6$, to the volume of an individual strand, $(m_b N_b + m_l)/(N_A \rho_{av})$, where N_A is Avogadro’s number, ρ_{av} is the average bulk density from DNA on planar surfaces, m_b is the molecular weight of a base, and m_l is the molecular weight of the thiol linkage. Dividing the number of strands by the surface area yields $\sigma = N_A \rho_{av} [(D + H)^3 - D^3]/[6D^2(m_b N_b + m_l)]$. With ρ_{av} of 0.89 to 1.3 g/cm³ reported for (dT)₂₅SH on a planar gold film by Petrovykh et al., $m_b = 304 \text{ g/mol}$, $m_l = 134 \text{ g/mol}$ for the six carbon thiol linked, and $N_b = 20$ or 30 bases, we find $\sigma = 9.0 \times 10^{12}$ to 6.4×10^{13} strands as compared to $\sigma = 2.0 \times 10^{12}$ to 4.0×10^{13} strands/cm² for the same

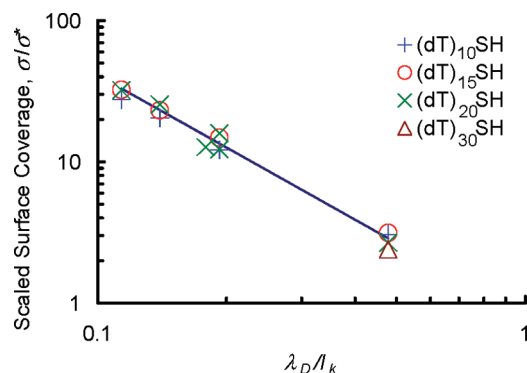


Figure 4. Scaled surface coverage, σ/σ^* , versus the ratio of the Debye length, λ_D , to the Kuhn length, l_k , where σ^* is inversely proportional to the molecular footprint of an individual, nonoverlapping strand, $(\langle x^2 \rangle)^{-1}$. The line represents a best fit of $\sigma/\sigma^* = 0.82(\lambda_D/l_k)^{-1.7}$.

conditions with the previous method.¹⁸ Thus, where the bulk density on similar surfaces prepared at similar salt concentrations is known this alternative approach may find utility, while the previous method may be more useful where Kuhn or persistence lengths are known.

The relationship between the surface coverage and the salt concentration, n_s , of the solutions used for ssDNA adsorption is shown in Figure 3. Scaling the surface coverage with the molecular footprint of a nonoverlapping strand collapses the data onto a single curve in Figure 4 and emphasizes the importance of the Debye length, $\lambda_D \sim n_s^{-1/2}$. Because DNA in solution is highly charged, strands anchored to the surface repel incoming strands due to charge–charge repulsion, that is, through excluded volume effects.^{16,17} Decreasing the Debye length, λ_D , by increasing the ionic strength moderates this repulsion, allowing DNA to pack more tightly on the surface. An increase in the salt concentration accordingly leads to higher surface coverages as demonstrated in Figure 3. In addition, the figure shows the surface coverage to scale with the Debye length to the -1.7 power. Similarly, the force exerted by the negatively charged strand anchored to the surface on incoming strands repels in both directions along the surface. This argument provides a comparable exponent of -2 , one for each axis in the plane of the particle surface.

We further consider the impact of the dried salts on the coating. Despite the possibility of dried salts further affecting the coating thickness beyond Kaufman's volumetric correction, this effect was not observed. Examination of the residuals (the salt-corrected total coating thickness minus the square root dependence depicted in Figure 2) versus the diameter of the dry salt peak (i.e., the first peaks in Figure 1) indicates no clear trend, and all residuals were within the diameter uncertainty. Accordingly, we believe the simple volumetric correction of

Kaufman adequately accounts for the presence of the salt, despite “crusts” ranging from approximately 0.1 to 1.2 nm in thickness.⁹ However, we cannot distinguish with this technique whether the crust lies on the top of the strands, at the base of the strands, or uniformly coats the strands, though the latter seems more likely.

In summary, these results indicate the potential of ES-DMA to quantify the coverage and configuration of biological molecules and organic coatings on nanoparticles. We considered the specific example of thiol-modified ssDNA and find it adopts a random coil configuration. We believe the analytical model to be valid generally for sufficiently long and flexible molecules (i.e., where $N_b \gg N_k$).

Acknowledgment. L.F.P. acknowledges support of a post-doctoral fellowship through the National Research Council. We express appreciation for helpful conversations with David L. Lahr, Joshua L. Hertz, Jack F. Douglas, and Mark A. Sobolewski.

Supporting Information Available: Details of the sample preparation and data analysis. This material is available free of charge via the Internet at <http://pubs.acs.org>.

References and Notes

- (1) Qin, W. J.; Yung, L. Y. L. *Biomacromolecules* **2006**, *7*, 3047.
- (2) Berry, C. C.; Curtis, A. S. G. *J. Phys. D: Appl. Phys.* **2003**, *36*, R198.
- (3) Demers, L. M.; Mirkin, C. A.; Mucic, R. C.; Reynolds, R. A.; Letsinger, R. L.; Elghanian, R.; Viswanadham, G. *Anal. Chem.* **2000**, *72*, 5535.
- (4) Xu, J.; Craig, S. L. *Langmuir* **2007**, *23*, 2015.
- (5) Liao, Y. C.; Roberts, J. T. *J. Am. Chem. Soc.* **2006**, *128*, 9061.
- (6) Bacher, G.; Szymanski, W. W.; Kaufman, S. L.; Zollner, P.; Blaas, D.; Allmaier, G. *J. Mass Spectrom.* **2001**, *36*, 1038.
- (7) Saucy, D. A.; Ude, S.; Lenggoro, I. W.; de la Mora, J. F. *Anal. Chem.* **2004**, *76*, 1045.
- (8) Loo, J. A.; Berhane, B.; Kaddis, C. S.; Wooding, K. M.; Xie, Y. M.; Kaufman, S. L.; Chernushevich, I. V. *J. Am. Soc. Mass Spectrom.* **2005**, *16*, 998.
- (9) Kaufman, S. L. *Anal. Chim. Acta* **2000**, *406*, 3.
- (10) Kimura-Suda, H.; Petrovykh, D. Y.; Tarlov, M. J.; Whitman, L. J. *J. Am. Chem. Soc.* **2003**, *125*, 9014.
- (11) AdamutiTrache, M.; McMullen, W. E.; Douglas, J. F. *J. Chem. Phys.* **1996**, *105*, 4798.
- (12) Russel, W. B.; Saville, D. A.; Schowalter, W. R. *Colloidal Dispersions*; Cambridge University Press: New York, 1989.
- (13) Netz, R. R.; Andelman, D. *Phys. Rep.* **2003**, *380*, 1.
- (14) Kent, M. S.; Lee, L. T.; Factor, B. J.; Rondelez, F.; Smith, G. S. *J. Chem. Phys.* **1995**, *103*, 2320.
- (15) Mansfield, M. L.; Douglas, J. F.; Irfan, S.; Kang, E. H. *Macromolecules* **2007**, *40*, 2575.
- (16) Tinland, B.; Pluen, A.; Sturm, J.; Weill, G. *Macromolecules* **1997**, *30*, 5763.
- (17) Rief, M.; Clausen-Schaumann, H.; Gaub, H. E. *Nat. Struct. Biol.* **1999**, *6*, 346.
- (18) Petrovykh, D. Y.; Perez-Dieste, V.; Opdahl, A.; Kimura-Suda, H.; Sullivan, J. M.; Tarlov, M. J.; Himpfel, F. J.; Whitman, L. J. *J. Am. Chem. Soc.* **2006**, *128*, 2.